

Synthesis, Processing, and Composition of the Virion-associated HTLV-1 Reverse Transcriptase*

Received for publication, July 14, 2005, and in revised form, December 12, 2005. Published, JBC Papers in Press, December 19, 2005, DOI 10.1074/jbc.M507660200

Michael S. Mitchell[‡], József Tözsér[§], Gerald Princler[‡], Patricia A. Lloyd[¶], Ashleigh Auth[‡], and David Derse^{‡1}

From the [‡]HIV Drug Resistance Program, NCI-Frederick, Frederick, Maryland 21702, [§]Department of Biochemistry, Medical University of Debrecen, H-4012 Debrecen, Hungary, and [¶]Basic Research Program, SAIC-Frederick, Frederick, Maryland 21702

It is not known whether the low infectivity and low virion-associated polymerase activity of human T-cell lymphotropic virus type-1 (HTLV-1) are due to the quantity or quality of the reverse transcriptase (RT), because the protein has not yet been fully characterized. We have developed anti-RT antibodies and constructed HTLV-1 expression plasmids that express truncated or hemagglutinin-tagged Pol polyproteins to examine the maturation and composition of HTLV-1 RT. We detected virion-associated proteins corresponding to RT-integrase (IN) (p98) and RT (p62) as well as smaller proteins containing the polymerase (p49) or RNase H domains. We have identified the amino acid sequences in the Pol polyprotein that are cleaved by HTLV-1 protease to yield RT and IN. We have also identified the cleavage sites within RT that give rise to the p49 polymerase fragment. Immunoprecipitation of an epitope-tagged p62 subunit coprecipitated p49, indicating that the HTLV-1 RT complex can exist as a p62/p49 heterodimer analogous to the RT of HIV-1 (p66/p51).

Human T-cell lymphotropic virus type-1 (HTLV-1)² is an oncogenic retrovirus belonging to the deltaretrovirus genus, which includes HTLV-2, -3, and -4, simian T-cell lymphotropic viruses, and bovine leukemia virus. As with many other retroviruses, HTLV-1 uses ribosomal frameshifting to regulate the relative expression of Gag proteins and the viral replication enzymes. In many retroviruses, including human immunodeficiency virus (HIV) and Rous sarcoma virus (RSV), protein synthesis that initiates from the *gag* start codon gives rise to both Gag and Gag-Pol polyprotein precursors. A ribosomal frameshift site encoded either at the 5'-end of *pol* (HIV) or at the 3'-end of *gag* (RSV) allows the synthesis of the Gag-Pol polyprotein (1, 2). In contrast, the *pro* gene of some retroviruses, such as HTLV, mouse mammary tumor virus, and Mason-Pfizer monkey virus, is in a separate reading frame from both *gag* and *pol*. Thus, the expression of Gag-Pol polyprotein in these retroviruses involves two ribosomal frameshifts: one where *gag* and *pro* overlap and the second within the *pro/pol* overlap (3–11). In these viruses, three polyprotein precursors are synthesized. In HTLV-1, they are Gag (Pr53), Gag-Pro (Pr76), and Gag-Pro-Pol (Pr180). Based on *in vitro* translation of viral RNA, the molar ratio of the Gag, Gag-Pro, and Gag-Pro-Pol polyproteins was estimated to be about 100:10:1 (12). This means that the relative amounts of Pol to Gag produced by

HTLV-1 would be 5–10-fold less than the amount present in single-frameshift retroviruses, such as HIV and RSV (1, 2) and 3–4-fold less than the amount found in the other two-frameshift retroviruses: mouse mammary tumor virus and Mason-Pfizer monkey virus (13–15).

Retroviral *pol* genes encode RT and integrase (IN), which are required for the replication and integration of the viral genome. The Pol precursor is enzymatically cleaved by the viral protease to yield the subunits of the RT complex. The reverse transcriptases of HIV-1, RSV, and murine leukemia virus are the prototypes of three distinct forms of RT (16). The heterodimeric RSV RT consists of an RT-IN β subunit and the RT α subunit (17). HIV-1 RT is a smaller heterodimer, where the larger subunit (p66) contains both polymerase and RNase H domains, and the smaller subunit (p51) corresponds closely, but not exactly, to the polymerase domain (18–22). In contrast to the RTs of HIV and RSV, the RT of murine leukemia virus is a monomer in solution, although it may dimerize when it binds nucleic acid (23, 24).

Shortly after the virus was identified in 1980, some basic properties of the virion-associated HTLV-1 RT were defined. The virion-associated enzyme had DNA polymerase and RNase H activity and was reported to have a molecular mass of about 95 kDa (25). However, neither the Pol cleavage products present in HTLV-1 virions nor their quaternary organization in the RT complex are known. Sequence alignments of diverse retroviral *pol* genes have been used to try to predict the HTLV-1 polymerase, ribonuclease H, and integrase functional domains (26–28), and based on these predictions, attempts were made to express recombinant HTLV-1 RT (28, 29). However, these sequence alignments did not correctly predict the N terminus of HTLV-1 RT. We recently demonstrated that the N-terminal residue of RT is not encoded immediately adjacent to the C terminus of protease (PR), as it is in other retroviruses (28, 30, 31). Instead, there is an 8-amino acid peptide, p1, that separates PR and RT. Removal of p1 from the C terminus of PR is not required for proteolytic activity, but removal of p1 from the N terminus of RT is essential for virion-associated RT activity and infectivity (30).

In order to define HTLV-1 Pol processing and to characterize the mature RT, we constructed virus expression plasmids that generate VLPs containing ~10-fold higher levels of Pol than wild-type virions. Immunoblotting of VLPs from transfected cells revealed Pol cleavage products corresponding to RT-IN, RT (p62), polymerase (p49), and RNase H (p15). Pol maturation was analyzed by immunoblotting proteins from wild type and mutant VLPs. Protease cleavage sites within Pol were then mapped by mutagenesis or by *in vitro* PR cleavage reactions. Immunoprecipitation of an epitope-tagged version of p62 RT from HTLV-1 VLPs co-precipitated the untagged p49 polymerase subunit, suggesting that the virion-associated HTLV-1 RT can exist as a p62/p49 heterodimer, analogous to the HIV-1 p66/p51 RT complex.

MATERIALS AND METHODS

Plasmids—pCMVHT-1 Δ env is an HTLV-1 expression plasmid that produces virus-like particles (VLPs) that lack the Env glycoprotein when

* The costs of publication of this article were defrayed in part by the payment of page charges. This article must therefore be hereby marked "advertisement" in accordance with 18 U.S.C. Section 1734 solely to indicate this fact.

¹ To whom correspondence should be addressed: National Cancer Institute, P.O. Box B, Bldg. 535/134, Frederick, MD 21702. Tel.: 301-846-5611; Fax: 301-846-6863; E-mail: derse@ncifcrf.gov.

² The abbreviations used are: HTLV, human T-cell lymphotropic virus; HIV, human immunodeficiency virus; RSV, Rous sarcoma virus; RT, reverse transcriptase; IN, integrase; PR, protease; VLP, virus-like particle; MA, matrix protein; HA, hemagglutinin; Bis-Tris, 2-[bis(2-hydroxyethyl)amino]-2-(hydroxymethyl)propane-1,3-diol; MES, 2-(*N*-morpholino)ethanesulfonic acid; MOPS, 3-(*N*-morpholino)propanesulfonic acid; RH, ribonuclease H.

the plasmid is transfected into cultured cells (32). pCMVHT-1 Δenv -polfs was constructed from pCMVHT-1 Δenv by inserting a deoxycytidine residue into the *pro/pol* ribosomal frameshift site using site-directed mutagenesis. This mutant plasmid expresses the HTLV-1 Gag-Pro-Pol polyprotein precursor via a single frameshifting event. The level of Gag-Pro-Pol expression is about 10-fold higher than from the parent HTLV-1 plasmid. Unless otherwise indicated, the following Pol mutations were constructed in the pCMVHT-1 Δenv -polfs backbone. Pol is 880 amino acids long, and our numbering of the 880-amino acid Pol is based on the N terminus of RT having the sequence GLEHLP (30). The IN Δ mutation creates a stop codon at amino acid 718; the RHA Δ mutation creates a stop codon at amino acid 514; and the RT Δ mutation creates a premature stop codon at amino acid 311. The F442am mutation creates a stop codon at amino acid residue 442 of Pol. An 11-amino acid hemagglutinin (HA) epitope tag followed by a stop codon was inserted after amino acid 581 to construct the RH-HA vector; the HA tag is inserted immediately upstream of the predicted RT/IN cleavage site. An HA tag was also inserted after amino acid residue 738, in the integrase domain, to make IN-HA. To construct the IN-HA-*psite* plasmid, the amino acids at the predicted RT/IN cleavage site (residues 582–585 of Pol) were changed from VLQL to GAQA.

Cell Lines, Transfections, and Preparation of Virus-like Particles—The human kidney line 293T was maintained in Dulbecco's modified Eagle's medium, supplemented with 10% fetal bovine serum, L-glutamine, and antibiotics. Virus stocks were generated by transfection of 293T cells with expression plasmids by calcium phosphate co-precipitation. The culture medium was replaced 16 h after transfection with Advanced Dulbecco's modified Eagle's medium, supplemented with 2% ultralow IgG fetal bovine serum, GlutaMAX-1, and antibiotics. Virus-containing supernatants were collected 24 h later. Transfected cell supernatants were cleared by low speed centrifugation and filtered through 0.45- μ m pore size low protein-binding filters (Millipore). VLPs were concentrated by ultracentrifugation through a 20% glycerol cushion in a Ti70 rotor at 30,000 rpm for 90 min at 4 °C.

The HTLV-1 transformed T-cell lines, MT-2, C10/MJ, and C8166 were maintained in RPMI 1640 and 10% fetal bovine serum. MT-2 and C10/MJ cells produce HTLV-1 virions, and C8166 does not. Cells were pelleted and resuspended in AIM-V medium (supplemented with 2% fetal bovine serum), and virus stocks were harvested after 24 h. Supernatants were cleared by low speed centrifugation and filtered through 0.45- μ m pore size low protein-binding filters. Virus particles were collected by ultracentrifugation, as described above.

Antibodies—A 15-amino acid-long synthetic peptide, NH₂-Cys-SENKTQQTPGTIKF-COOH (ProSci, Inc.), which contained a cysteine residue at the amino terminus and amino acid residues 204–217 of the mature HTLV-1 RT, was used to raise rabbit antiserum designated as anti-RT^M. An aliquot of the affinity-purified antibody was biotinylated (Molecular Probes, Inc., Eugene, OR) and used to detect immunoprecipitated Pol products. In addition, a previously described rabbit polyclonal antibody that recognizes amino acids 4–16 of HTLV-1 RT, designated as anti-RT^N, was used to detect Pol products (30). Hemagglutinated Pol products were immunoprecipitated with an agarose-conjugated anti-HA antibody (Covance clone 16B12). A rat monoclonal antibody (Roche Applied Science clone 3F10) was used for chemiluminescent detection of immunoprecipitated HA-tagged protein. A mouse monoclonal antibody (Santa Cruz Biotechnology, Inc. (Santa Cruz, CA) clone F-7 or Covance clone 16B12) was used to detect the epitope-tagged Pol products on Western blots of VLP lysates. A mouse monoclonal antibody (Zeptomatrix clone 46/6.11.1.3) specific for HTLV-1 MA (p19) was used to monitor Gag processing.

Immunoblotting—VLPs were lysed in LDS sample buffer (Invitrogen) and denatured under reducing conditions prior to separation on 4–12% Bis-Tris gels in MES buffer or 10% Bis-Tris gels in MOPS buffer. Proteins were transferred to Immobilon-P (Millipore) membranes for immunodetection. In most cases, blots were probed with a horseradish peroxidase-conjugated secondary antibody and visualized by chemiluminescence. Blots of immunoprecipitated proteins were probed with biotinylated anti-RT^M and detected by avidin-horseradish peroxidase and chemiluminescent staining.

Immunopurification—VLPs were lysed in LDS sample buffer (Invitrogen). One-fifth of the volume was reserved for analysis by Western blotting, and the remaining lysate was diluted 20-fold in radioimmune precipitation buffer. The viral lysates were precleared with agarose-conjugated normal mouse IgG for 1 h at room temperature and then incubated overnight with agarose-conjugated mouse anti-HA (Covance). After the overnight incubation, the agarose beads were washed five times with radioimmune precipitation buffer before eluting bound protein with LDS sample buffer. The VLP lysate and immunopurified samples were heated at 70 °C for 10 min under reducing conditions, loaded onto a 10% Bis-Tris polyacrylamide gel, and separated at 150 V in MOPS buffer. Proteins were transferred to an Immobilon P membrane (Millipore), probed with biotinylated anti-RT^M, and detected by avidin-horseradish peroxidase and chemiluminescent staining.

In Vitro RT Assays—Reverse transcriptase assays were performed with a bacteriophage MS2 RNA template and a corresponding primer. The template-primer was prepared by combining equimolar amounts of MS2 RNA (Roche Applied Science) and RT-1 DNA primer (5'-GGAAGAACTCTTGAAGGTG-3') in 20 mM Tris-HCl, pH 8.0, plus 0.1 mM EDTA. The template-primer was annealed by heating at 95 °C for 5 min and then at 37 °C for 30 min, followed by the addition of 200 units of RNasin (Promega) or SUPERase-In (Ambion). RT reactions were carried out in a final volume of 25 μ l containing 20 μ l of RT buffer (50 mM Tris-HCl, pH 8.3, 75 mM KCl, 3 mM MgCl₂, 10 mM dithiothreitol, and 100 μ M dNTPs) plus 2 μ l (0.245 pmol) of MS2 RNA template-primer and 3 μ l of virion extract. Reactions were incubated for 3 min at 37 °C followed by heating at 95 °C for 7 min. Virion extracts were prepared by centrifugation of cell culture supernatants and lysis of the virion pellet in RT extraction buffer (50 mM Tris-HCl, pH 8.0, 100 mM NaCl, 0.1 mM EDTA, 20 mM dithiothreitol, 0.2% Nonidet P-40, 20% glycerol, and 0.1 mg/ml bovine serum albumin) for 15 min on ice. The DNA products were quantified by Taqman real time PCR analysis.

Real time PCR quantitation of the RT reaction products was performed on a Prism 7700 sequence detector (PerkinElmer Life Sciences/Applied Biosystems). 25- μ l PCRs contained 5 μ l of the RT reaction plus 20 μ l of Taqman master mix (Applied Biosystems), containing 100 ng of RT-2 primer (5'-CCTAAACGAAGATCGAAAGT-3'), 100 ng of RT-3 primer (5'-AACCTTCGTAAGCATCTCAT-3'), 100 ng of Taqman probe (5'-carboxyfluorescein-TGAGTGATATCCAGGGTGC-6-carboxytetramethylrhodamine-3'), 0.02 units of RNase H (Invitrogen), 0.0005 units of RNase A, and 0.02 units of RNase T1 (Ambion). Reactions were incubated at 37 °C for 30 min to degrade any residual RNA that could serve as a template for Taq polymerase (33, 34). The PCR amplification conditions were 50 °C for 2 min followed by 95 °C for 10 min to activate the DNA polymerase and then 50 cycles of 15 s at 94 °C and 1 min at 60 °C. Calibration curves were derived with a pCR-II TOPO plasmid containing a cDNA segment of the MS2 genome (nucleotides 21–790; GenBankTM accession number V00642), which was serially diluted over the range of 2.5 \times 10⁰ to 2.5 \times 10⁷ molecules, as previously described (35). RT activity is expressed as the number of

Characterization of HTLV-1 Reverse Transcriptase

cDNA molecules generated under these reaction conditions per pg of Gag protein added to the reaction. The HTLV-1 p19 (MA) enzyme-linked immunosorbent assay kit from Zeptomatrix was used to quantify the Gag protein.

In Vitro Cleavage of Synthetic Peptides—Oligopeptides were obtained from Biosynthesis Inc. (Lewisville, TX). Stock solutions and dilutions were made in distilled water, and the peptide concentrations were determined by amino acid analysis with a Beckman 6300 amino acid analyzer. Stabilized, purified HTLV-1 PR was prepared as described previously (36). Active site titration of the PR was performed using peptide KTKVL-r-VVQPK (IB268), where r represents a reduced peptide bond, as described previously (37). The PR assays were initiated by the mixing of 5 μ l (34–1700 nM) of purified HTLV-1 PR with 10 μ l of 2 \times incubation buffer (0.5 M potassium phosphate buffer, pH 5.6, containing 10% glycerol, 2 mM EDTA, 10 mM dithiothreitol, 4 M NaCl) and 5 μ l of 0.04–1.2 mM substrate. The reaction mixture was incubated at 37 $^{\circ}$ C for 1 h or overnight, and the reaction was stopped by the addition of 180 μ l of 1% trifluoroacetic acid, and an aliquot was injected onto a Nova-Pak C₁₈ reversed-phase chromatography column (3.9 \times 150 mm; Waters Associates, Inc.) using an automatic injector. Substrates and the cleavage products were separated using an increasing water-acetonitrile gradient (0–100%) in the presence of 0.05% trifluoroacetic acid. Cleavage product peaks were collected and were identified by mass spectrometric analysis and by amino acid analysis, which was also used to quantify the amount of products generated. Due to the estimated low K_m value, the k_{cat}/K_m value for the most efficiently cleaved peptide was determined using a competition assay performed in triplicate, as previously described for several HTLV-1 PR substrates (38).

RESULTS

Pol Synthesis and Predicted Cleavage Products—Expression of HTLV-1 Pol requires that two ribosomal frameshifts occur during translation of viral mRNA. Neither frameshift is efficient; translation produces Gag, Gag-Pro, and Gag-Pro-Pol polyprotein precursors in a ratio of about 100:10:1 (Fig. 1A). These polyproteins assemble into an immature virion; maturation of the virion by proteolytic processing is predicted to produce a 98-kDa Pol precursor, containing the p1, polymerase, ribonuclease H, and integrase domains. Removal of p1 is required for virion-associated RT activity and virus replication (30). There is a predicted processing site at the junction of the RNase H and integrase domains that would produce an IN protein of \sim 33 kDa. The combined molecular mass of the polymerase and ribonuclease H domains is estimated to be about 64 kDa. If cleavage were also to occur between the polymerase and RNase H domain in HTLV-1 RT, similar to the cleavage that takes place in HIV-1 RT, the resulting peptides would be \sim 50 and 14 kDa, respectively.

The small amount of mature RT present in virions makes it difficult to detect virion-associated HTLV-1 RT. Similar difficulties have been encountered in investigations of the RTs of mouse mammary tumor virus and Mason-Pfizer monkey virus, which also use two ribosomal frameshifts to express Pol (39). We increased the expression of Gag-Pro-Pol in HTLV-1 VLPs by inserting a base pair into the second ribosomal frameshift site to create the polfs construct: pCMVHT Δ env-polfs (Fig. 1A) (30). This insertion mutation places the *pro* and *pol* open reading frames in the same reading frame, increasing the production of Gag-Pro-Pol and eliminating the expression of Gag-Pro. Polfs constructs efficiently produce VLPs in which Gag is processed normally (30).

Rabbit antiserum was raised against a peptide in the *pro/pol* trans-frame protein (p9), whose sequence corresponds to amino acids 4–16 of

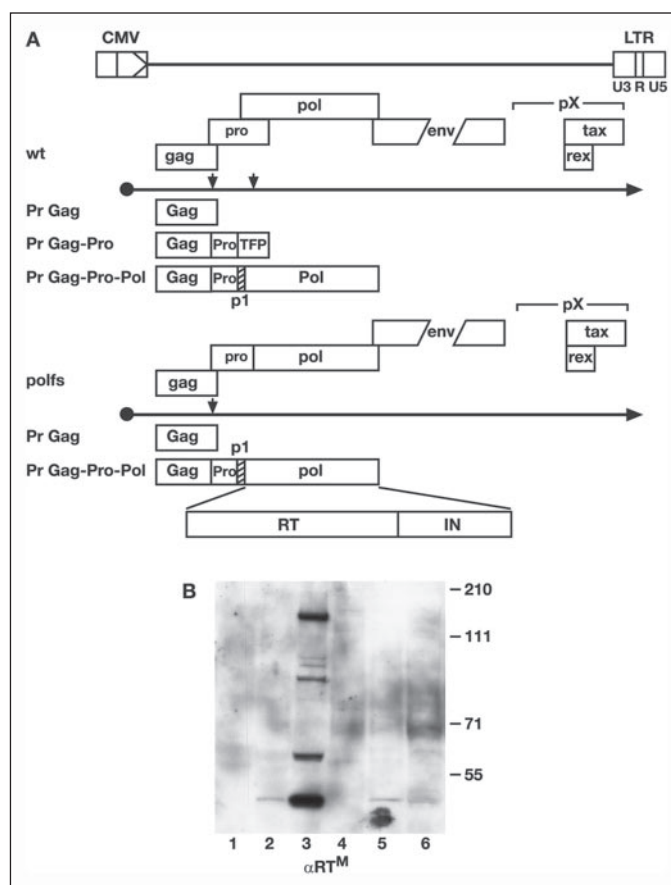


FIGURE 1. HTLV-1 virion- and VLP-associated Pol proteins. A, major structural features of the wild-type (*wt*) and polfs HTLV-1 expression plasmids are shown with their respective primary mRNAs and the polyproteins that are generated from the *gag* initiation codon. The locations of the major genes are shown below the viral genome. The arrows mark the ribosomal frameshift sites on the viral mRNAs. The polyproteins are indicated below the mRNA transcripts and reflect whether zero, one, or two frameshifts occur during translation. The proteins present in Pol are indicated at the bottom. B, immunoblot showing RT-reactive proteins present in virions from transfected cells (lanes 1–3) or HTLV-1 transformed cell lines (lanes 4–6). Lane 1, mock transfection; lane 2, 293T/pCMVHT-1; lane 3, 293T/pCMVHT-1 Δ env-polfs; lane 4, C8166; lane 5, MT-2; lane 6, C10/MJ. Virus particle concentrations were quantified by HTLV-1 p19 (MA) enzyme-linked immunosorbent assay to normalize loading. Blots were probed with affinity-purified anti-RT^M antibody. The molecular masses of the prestained size markers are indicated in kilodaltons on the right. It should be noted that the migration of the Pol products relative to molecular size markers on the 7% Tris acetate gel used in this experiment is different than the relative migration of these proteins on NuPAGE Bis-Tris gels in MES and MOPS buffer used in other figures.

the mature RT; this antiserum is designated anti-RT^N (30). In addition, we recently made an antiserum, designated as anti-RT^M, against a peptide corresponding to residues 204–217 of the mature HTLV-1 RT. Fig. 1B shows an immunoblot of HTLV-1 proteins from VLPs derived from transfected 293T cells and from virions released by productively infected T-cell lines probed with the anti-RT^M antibody. Specific bands were not detected in supernatant from mock-transfected 293T cells (lane 1) or from C8166 T-cells, which do not produce HTLV-1 structural proteins (lane 4). A single band migrating at \sim 49 kDa was detected in VLPs from 293T cells transfected with HTLV-1 expression plasmids (lane 2) and from chronically HTLV-1-infected T-cell lines, MT-2 (lane 5) and C10/MJ (lane 6). VLPs from 293T cells transfected with the polfs construct contained significantly more Pol proteins than wild-type VLPs, as evidenced by the intensity of the protein bands in lane 3. Although the p49 band was the most intense, other bands can be seen that migrate at 163, 98, and 62 kDa, consistent with the predicted sizes for Gag-Pro-Pol, RT-IN, and RT, respectively. Immunoblots probed

TABLE 1
Virion-associated RT activity

Virus-like particles were concentrated from supernatants of 293T cells transfected with wild type or mutant HTLV-1 expression plasmids. VLP lysates were added to RT reactions containing an MS2 RNA template-primer. The amount of MS2 RNA converted to cDNA was quantified by Taqman real time PCR analysis as described under "Materials and Methods." RT activity is expressed as an average of the number of molecules of cDNA produced/pg of Gag in the RT reaction with S.E.

	Average RT/pg
pCMVHT-1 Δenv	2.2 \pm 0.83
pCMVHT-1 Δenv -polfs	2.8 \pm 0.78
pCMVHT-1 Δenv -polfs IN-HA	1.2 \pm 0.11
pCMVHT-1 Δenv -polfs IN-HA-psite	1.0 \pm 0.16
pCMVHT-1 Δenv -polfs RH-HA	6.0 \pm 1.8
pCMVHT-1 Δenv -polfs Δ RH	0.0068 \pm 0.0067
pCMVHT-1 Δenv -polfs F442am	0.00053 \pm 0.00028
pUC19	0

with the anti-RT^N antibody gave similar results. None of these Pol products were detected in immunoblots of proteins from VLPs with a mutated protease (data not shown). Although the polfs mutation resulted in a significantly higher amount of Pol products in VLPs, the polymerase activity associated with these virions is (at best) only about 2–3-fold higher than the polymerase activity associated with wild-type virions rather than the 10-fold higher activity that might be expected (Table 1).

Characterization of the Pol Cleavage Products—To identify the Pol cleavage products observed in the immunoblots of HTLV-1 virus and VLPs, we transfected 293T cells with a series of pCMVHT-1 Δenv -polfs constructs encoding truncated versions of the Gag-Pro-Pol polyprotein (Fig. 2A). Stop codons were introduced into the integrase, ribonuclease H, or polymerase regions of *pol*; these will shorten the Gag-Pro-Pol polyprotein by 163 (IN Δ), 368 (RH Δ), or 572 (RT Δ) residues. Immunoblots of the VLP lysates were probed with anti-RT^N antibody (Fig. 2B) or with anti-p19 (MA) antibody (Fig. 2C).

Immunoblots probed with anti-RT^N antibody showed that VLP lysates from cells transfected with pCMVHT-1 Δenv -polfs (designated here as wild type) produce bands of ~163, 98, 62, and 49 kDa and a smaller band of about 17 kDa (Fig. 2B, lane 1); as seen previously, the p49 band was the most intense. The 163-kDa band, which is Gag-Pro-Pol, shows an appropriate decrease in size in the IN Δ (lane 2), RH Δ (lane 3), and RT Δ (lane 4) mutations. As expected, these high molecular weight bands were detected with the anti-p19 (MA) antibody (Fig. 2C). The band in lane 1 running at ~98 kDa is RT-IN; its size is decreased to ~80 kDa in the IN Δ mutant (lane 2). The p62 band corresponds to RT, since it was not affected by the IN Δ mutation, but it was reduced to ~57 kDa in the RH Δ VLPs. The p49 protein was present in all VLPs except those from the RT Δ mutant, which caused this band to shift to ~35 kDa. The p49 protein is derived by the proteolytic cleavage of RT-IN or p62 RT, and it contains the N terminus of RT, because the anti-RT^N antibody recognizes it. Likewise, the band migrating at ~17 kDa, which appears to be present in all VLPs except RT Δ , is believed to be an N-terminal fragment of RT.

We monitored the effects of the Pol truncations on HTLV-1 Gag processing, because it has been reported that truncations of the HIV-1 *pol* domain impair and interfere with proper virion assembly, release, and maturation of virus particles (40, 41). Although the polfs mutation resulted in the accumulation of more pr53 Gag polyprotein precursor compared with wild-type VLPs, the Pol truncations did not cause Gag processing defects or appear to affect the packaging of Gag-Pro-Pol in VLPs (Fig. 2C). *In vitro* reverse transcription of bacteriophage MS2 RNA, quantified by Taqman real time PCR, was used to measure the level of virion-associated RT activity of the Pol truncation mutants (described below). As expected, the truncation (Δ RH) or deletion

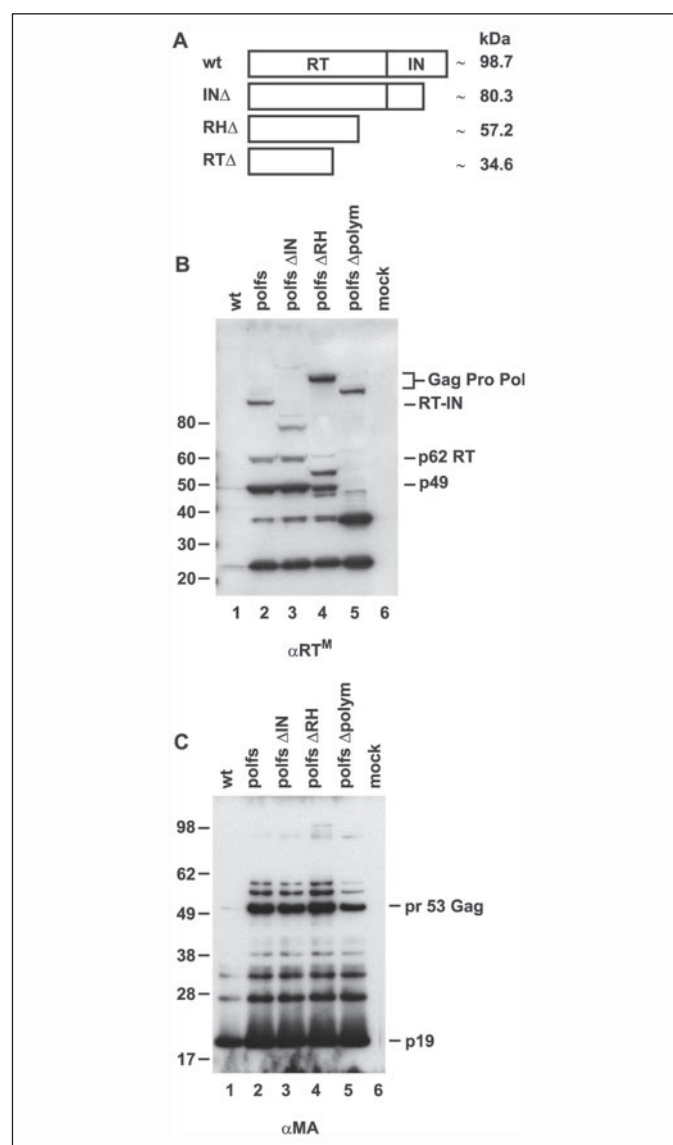


FIGURE 2. Identification of the Pol cleavage products present in HTLV-1 VLPs. A, stop codons were inserted into the *pol* gene to generate truncated Pol proteins. The estimated sizes of the resulting Pol proteins are shown. B, VLPs from 293T cells transfected with various pCMVHT-1 Δenv -polfs expression plasmids were fractionated by SDS-PAGE on a 4–12% Bis-Tris gel in MOPS buffer and immunoblotted with anti-RT^N antibody. Lane 1, wild type (wt); lane 2, polfs; lane 3, polfs Δ IN; lane 4, polfs Δ RH; lane 5, polfs Δ RT; lane 6, mock transfection. C, a parallel immunoblot of the same samples as in B was run in MES buffer and probed with anti-p19 (MA) antibody. The molecular masses of the MagicMark (B) and prestained size markers (C) are indicated to the left of each panel, and the viral proteins are indicated on the right.

(F442am) of the RNase H domain eliminated the polymerase activity of RT (Table 1). The absence of a full-length integrase domain (Δ IN, IN-HA, IN-HA-psite, and RH-HA) had no noticeable effect on polymerase activity (data not shown for Δ IN). Furthermore, polymerase activity was not affected when a portion of the IN domain was fused to RT (IN-HA-psite) or when IN was replaced with an HA tag (RH-HA). These data indicate that Gag-Pro-Pol packaging into VLPs, Gag-Pro-Pol processing, and polymerase activity were not affected by the absence of the IN domain; nor did polymerase activity require cleavage of IN from RT.

RT-IN Cleavage—Sequence alignments suggested that the most likely site for RT-IN cleavage was ⁵⁸²VL↓QL⁵⁸⁵, with the scissile bond located between Leu⁵⁸³ and Gln⁵⁸⁴ (28, 30), although the recent *in vitro*

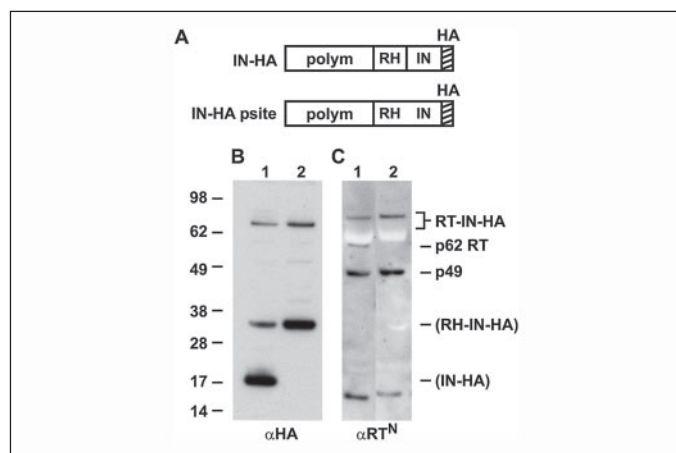


FIGURE 3. Mutation of the RT-IN protease cleavage site. *A*, schematic representation of the Pol precursors made by the IN-HA mutants. The polymerase (*polym*), RH, and IN domains of Pol are indicated. The IN-HA-psite construct has a mutation in the predicted protease cleavage site between RT and IN. *B*, VLPs obtained from supernatants of 293T cells transfected with pCMVHT-1Δ*env*-polfs-IN-HA (*lane 1*) or pCMVHT-1Δ*env*-polfs-IN-HA-psite (*lane 2*) were immunoblotted and probed with anti-HA antibody. Molecular masses of the prestained size markers are indicated in kilodaltons on the left. *C*, the same constructs as in *B* were immunoblotted and probed with anti-RT^N antiserum. The major Pol products are indicated on the right, with labels in parentheses denoting products appearing in *B*.

cleavage of a synthetic peptide with recombinant HTLV-1 protease suggested a slightly different, overlapping cleavage sequence, ⁵⁸⁴QL↓SP⁵⁸⁷ (42). To determine if ⁵⁸²VLQL⁵⁸⁵ is part of the *in vivo* RT-IN cleavage site, we inserted an HA epitope tag into the integrase region of the polfs construct to create IN-HA (Fig. 3A). In this construct, 142 amino acids at the C terminus of IN are replaced with an 11-amino acid HA epitope tag. The VLQL sequence of IN-HA was changed to GAQA to create the IN-HA-psite mutant (Fig. 3A). Immunoblots of VLPs produced by the IN-HA construct were probed with either anti-HA antibody or anti-RT^N antibodies to identify the N-terminal and C-terminal cleavage products. The unprocessed Pol precursor was ~75 kDa and was detected with both the anti-HA and anti-RT^N antibodies (Fig. 3, *B* and *C*). Cleavage between RNase H and IN domains produced the expected IN-HA fragment of 19 kDa, which was detected by anti-HA antibody (Fig. 3*B*, *lane 1*), and a 62-kDa RT fragment containing the polymerase and RNase H domains, which was detected with the anti-RT^N antibody (Fig. 3*C*, *lane 1*). The 19-kDa IN-HA peptide and 62-kDa RT were not observed in IN-HA-psite VLPs (Fig. 3*C*, *lane 2*), indicating that the VLQL to GAQA mutation prevented proteolytic cleavage. This suggests that the C terminus of RT is contained within the sequence ⁵⁸²VLQL⁵⁸⁵, although our data are unable to resolve whether the cleavage occurs between Leu⁵⁸³ and Gln⁵⁸⁴ (28) or between Leu⁵⁸⁵ and Ser⁵⁸⁸ (42).

In addition to the Pol cleavage products that correspond to RT (62 kDa) and IN-HA (19 kDa), a ~35-kDa band was detected with the anti-HA antibody (Fig. 3*B*, *lanes 1* and *2*) that is consistent with an RH-IN-HA fragment generated by cleavage within p62 RT. There is more of the RH-IN-HA cleavage product in the IN-HA-psite mutant VLPs compared with the IN-HA VLPs, presumably because this product cannot be cleaved to produce the 19-kDa IN-HA fragment. The expected N-terminal product from cleavage of the p62 RT at this site would be the 49-kDa polymerase protein, which was detected with the anti-RT^N antibody (Fig. 3*C*, *lanes 1* and *2*). In addition, the 17-kDa band, which we believe to be an N-terminal RT fragment produced by further cleavage of p49, was present in both the IN-HA and IN-HA psite VLPs.

Internal Cleavage of p62 RT—To examine the processing of p62 RT, we inserted a sequence encoding an HA epitope tag after Leu⁵⁸³, near

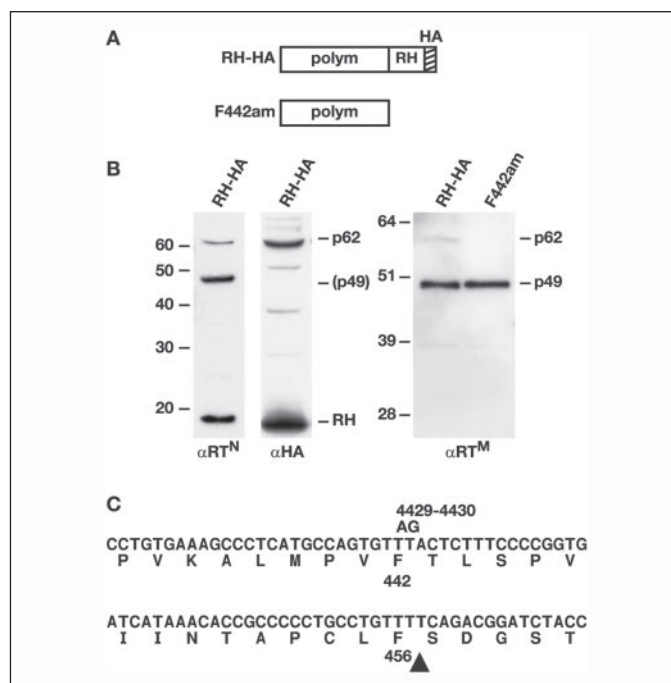


FIGURE 4. Protease cleavage site within p62 RT. *A*, schematic representation of the Pol precursors made by the RH-HA and F442am constructs. The polymerase (*polym*) and RH domains are indicated. *B*, the immunoblot on the left shows anti-RT^N-reactive material present in VLPs obtained from the supernatant of 293T cells transfected with the RH-HA mutant. The same blot, stripped and probed with monoclonal anti-HA antibody, is shown in the middle. The immunoblot to the right shows anti-RT^M-reactive material present in VLPs from cells transfected with the RH-HA and F442am mutants. *C*, the nucleotide and the predicted amino acid sequences of RT at the polymerase and ribonuclease H domain boundary are shown. The nucleotide changes used to introduce an amber stop codon into the RT coding sequence at Phe⁴⁴² are indicated above the sequence. The arrow indicates the cleavage site predicted by Trentin *et al.* (28).

the end of the RH domain, to construct RH-HA (Fig. 4A). Pol products in the RH-HA VLP lysates were examined by immunoblotting with anti-HA or anti-RT antibodies. Both the anti-HA and anti-RT^N antibodies detected unprocessed p62 RT protein (Fig. 4*B*). The anti-RT^N antibody also detected the 49- and 17-kDa proteins seen in Figs. 2*B* and 3*C*, whereas the anti-HA antibody detected a 15-kDa C-terminal cleavage product that would correspond to the HA-tagged RNase H domain. This 15-kDa cleavage product is analogous to the 35-kDa RH-IN-HA product observed in IN-HA VLP lysates (Fig. 3*B*), which contained about 20 kDa of IN-HA fused to the RNase H domain. Taken together, these data indicate that the 62-kDa RT protein is cleaved at an internal site to yield a 49-kDa N-terminal fragment comprising the polymerase domain and a 15-kDa C-terminal fragment comprising the RNase H domain.

Based on the apparent molecular weight of the p49 N-terminal protein and 15-kDa C-terminal fragment, we predicted the internal cleavage site to be between RT residues 440 and 450 (Fig. 4*C*). We converted Phe⁴⁴² to a stop codon to create the F442am provirus mutant (Fig. 4, *A* and *C*). Proteins from VLPs produced by F442am were run alongside proteins from RH-HA VLPs and immunoblotted with anti-RT^M antibody (Fig. 4*B*, right). The truncated RT protein detected in F442am VLPs always runs a fraction slower than p49, indicating that the internal cleavage site in wild-type RT is just upstream of Phe⁴⁴². To map the cleavage site(s) near Phe⁴⁴² that gives rise to an p49, we analyzed four oligopeptides as substrates for HTLV-1 PR in an *in vitro* cleavage assay. These peptides, D1 (KPVKALMPVFTLSK), D2 (KALMPVFTLSPVIK), D3 (KPVFTLSPVIINTK), and D4 (KVIINTAPCLFSDK), contain overlapping sequences from the RT polymerase/RNase H boundary and

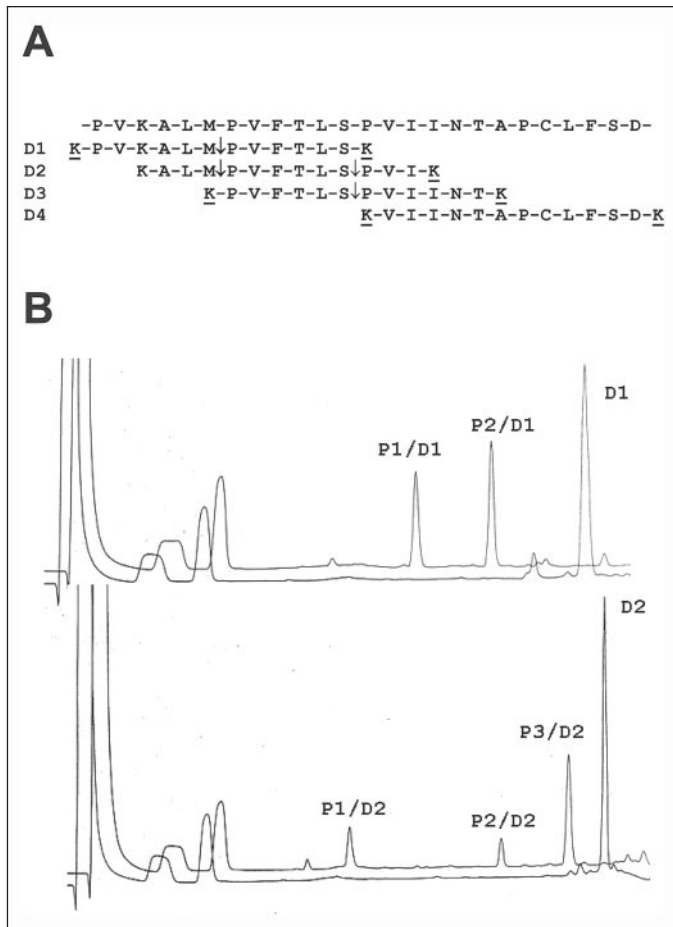


FIGURE 5. Determining p62 RT internal cleavage site using oligopeptides. *A*, amino acid sequence of HTLV-1 RT at the boundary between polymerase and ribonuclease H domains. The sequence of overlapping peptides D1–D4 that cover the region of interest are shown below the protein sequence derived from the cloned provirus. Lysine residues added to increase the solubility of peptides are *underlined*. The major and minor cleavage sites determined here are indicated with **boldface type** or *downward arrows*, respectively. *B*, high pressure liquid chromatography chromatograms of oligopeptides D1 and D2, which were incubated in the presence or absence of purified HTLV protease as described under “Materials and Methods.” Overnight incubation yielded complete cleavage of both peptides, yielding the following fragments identified by amino acid analysis and mass spectrometry: P1/D1 (KPVKALM), P2/D1 (PVFTLSK), P1/D2 (KALM), P2/D2 (PVFTLS), and P3/D2 (PVFTLSPVIK).

additional lysine residues at the termini (*underlined*) to improve solubility (Fig. 5*A*). Peptide D1 appeared to be a very efficient substrate of HTLV-1 PR, since it was completely cleaved into two fragments at the M ↓ P site (Fig. 5*B*). Peptide D2 was also hydrolyzed very efficiently, yielding three major identified fragments as a result of cleavage at both the M ↓ P and S ↓ P sites (Fig. 5*B*). Peptide D3 was hydrolyzed very inefficiently (less than 10%); overnight incubation yielded a small amount of KPVFTLS as cleavage product, indicating an inefficient cleavage at the S ↓ P site. Peptide D4 remained intact, even when it was incubated overnight with concentrated HTLV-1 PR (data not shown). An attempt was made to determine the kinetic parameters for peptide D1 using the Michaelis-Menten approach; however, due to its low K_m value, we were able to estimate only k_{cat} , which was $1.12 \pm 0.06 \text{ s}^{-1}$. The specificity constant (k_{cat}/K_m) was determined by competition assay using KTKIL ↓ VVQPK, which is an efficient substrate that has a k_{cat}/K_m of $63.1 \text{ mM}^{-1} \text{ s}^{-1}$ (38). This assay provided a k_{cat}/K_m of $95.9 \pm 6.5 \text{ mM}^{-1} \text{ s}^{-1}$ for peptide D1. These experiments show that a protease cleavage site within RT is an excellent substrate for HTLV-1 PR, which hydrolyzes the bond between Met⁴³⁹ and Pro⁴⁴⁰. This cleavage gives rise

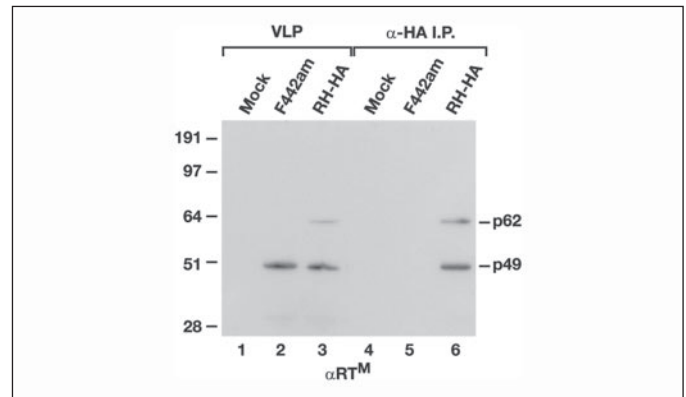


FIGURE 6. Immunoprecipitation of a p62/p49 complex. VLPs were prepared from 293T cells transfected with RH-HA or F442am mutants or from mock-transfected cells. A fraction of the VLP lysate was used directly for immunoblotting (*lanes 1–3*). The remainder was immunoprecipitated with anti-HA antibody-coated beads. After extensive washes, the p62 RT-HA protein bound to the beads was eluted and separated by SDS-PAGE and examined by immunoblotting with anti-RT^M antibody (*lanes 4–6*). Protein size markers are indicated on the *left*, and positions of p62 and p49 are shown to the *right*.

to the p49 peptide and a smaller fragment containing the RNase H domain.

Virion-associated RT Complex—To test the hypothesis that the HTLV-1 RT complex is a heterodimer of p62 and p49, we immunoprecipitated HA-tagged Pol products from RH-HA VLPs using anti-HA antibody-coated beads. If p62 RT is a monomer or homodimer, we would expect to purify only the HA-tagged p62; if HTLV-1 RT is a heterodimer, the untagged p49 subunit should co-purify with the HA-tagged p62 RT subunit. Virus-like particles were harvested from the supernatants of 293T cells transiently transfected with RH-HA or F442am DNA. The F442am mutant expresses only the untagged pseudo-p49 protein and served as a control for any nonspecific carryover of p49 through the immunoprecipitation.

Samples of VLP lysates or anti-HA immunoprecipitates were separated by SDS-PAGE, immunoblotted, and probed with biotinylated anti-RT^M antibody (Fig. 6). No bands were detected in concentrated supernatants from mock-transfected cells (*lanes 1 and 4*). As expected, VLPs from the F442am mutant contained the pseudo-p49 protein (*lane 2*), but this protein did not bind to the anti-HA beads (compare *lanes 2 and 5*). In contrast, p49 was detected in anti-HA immunoprecipitates of RH-HA VLPs (*lanes 3 and 6*), indicating an association between p49 and p62-HA. These results provide strong evidence in favor of HTLV-1 RT being a p62/p49 heterodimer. Despite the fact that the quantity of p49 detected in VLPs was often substantially greater than that of p62 (see Figs. 1*A*, 2*B*, 3*C*, 4*B*, and 6, *lane 3*), the p49/p62 ratio in immunoprecipitates was close to 1:1. The predicted size of the heterodimer is consistent with the published size (95 kDa) of the virion-associated RT activity (25).

DISCUSSION

Characterizing the maturation of virion-associated HTLV-1 Pol proteins is a necessary first step in determining if the postentry block to efficient HTLV-1 infection is related to the quantity or quality of RT. Defining the mature forms of HTLV-1 Pol proteins is also a prerequisite for producing recombinant RT for use in future structure-function analyses. The major barrier to analysis of Pol protein maturation is the very small amount of Pol that is packaged into HTLV-1 particles. However, the quantity of RT does not entirely account for the low infectivity of HTLV-1, because increasing the amount of Pol incorporated into VLPs did not improve infectivity (5) and only slightly increased virion-

Characterization of HTLV-1 Reverse Transcriptase

associated polymerase activity (Table 1). To detect Pol proteins in VLP lysates by immunoblotting, we mutated the second ribosomal frame-shift site in HTLV-1 expression vectors to significantly increase the amount of Pol incorporated into VLPs. We detected VLP-associated proteins corresponding to the Gag-Pol polyprotein, RT-IN, RT, and smaller RT cleavage products. The major Pol protein in lysates of VLPs from transfected cells or virions from chronically infected T-cell lines was not p62 RT but rather a 49-kDa protein containing the amino-terminal portion of p62 RT that encodes the polymerase domain.

The location of the protease cleavage site between RT and IN that has been identified here confirms the location predicted from amino acid sequence analysis (40) and *in vitro* peptide cleavage experiments (21). However, the usefulness of sequence analysis to predict cleavage sites involved in Pol maturation is limited. Sequence analysis was unable to predict the additional cleavage site between PR and RT that was previously shown to generate the amino terminus of RT (5) and RT sequence alignments did not predict the cleavage site within RT that is used to yield p49 (40). Trentin *et al.* (28) predicted that if cleavage occurred, the scissile bond would be located in the sequence ⁴⁵³LFSD⁴⁵⁶ between Phe⁴⁵⁴ and Ser⁴⁵⁵. Mutation of the LFSD sequence to AASD in the RH-HA provirus did not alter RT processing (data not shown). Initially, our studies indicated that the internal RT cleavage site was located in the vicinity of Pol amino acid position 440, because the native p49 fragment was just a bit larger than a protein expressed from the virus that encodes a stop codon at Phe⁴⁴², but attempts to sequence the immunoprecipitated RH-HA fragment suggested that a putative cleavage site might exist between Ser⁴⁴⁵ and Pro⁴⁴⁶. Four oligopeptides having overlapping sequences of the RT polymerase/RNase H boundary were tested as substrates of the HTLV-1 PR in an *in vitro* assay. A similar mapping strategy was previously successfully utilized to determine the cleavage site in the corresponding region of equine infectious anemia virus reverse transcriptase (43). Analysis of cleavage products identified a major cleavage site between Met³³⁹ and Pro⁴⁴⁰ and a substantially less efficient site between Ser⁴⁴⁵ and Pro⁴⁴⁶. Previous specificity studies of retroviral proteases established that the most important determinant of specificity is the P2–P2' region (nomenclature is according to Schechter and Berger (44)) of a substrate (45). Detailed specificity studies of HTLV-1 PR suggested that efficient cleavage sites require Leu, Ile, or Val at P2; Leu, Met or Phe at P1; Pro, Phe, Val, or Ala at P1'; and Leu, Ile, or Val at P2' (37, 38). The LM ↓ PV cleavage site conforms very well with these specificity determinants, whereas the inefficient LS ↓ PV site does not contain an optimal P1 residue. The cleavage of HTLV-1 p62 RT to generate p49 is reminiscent of the processing of the HIV-1 p66 RT subunit to produce the p51 subunit. The existence of p49 in HTLV-1 virions suggests that HTLV-1 RT could be a p62/p49 heterodimer, analogous to the p66/p51 RT heterodimer of HIV-1. Our immunoprecipitation results indicate that HTLV-1 RT can form a p62/p49 heterodimer; whether HTLV-1 RT functions as a heterodimer *in vivo* awaits further biochemical analysis.

HTLV-1 virions produced by transfected cells and chronically infected cell lines contained greater quantities of p49 polymerase than the p62 RT protein, which may contribute to the low enzymatic activity of virion-associated RT. In contrast, HIV-1 Pol processing is regulated so that p66 and p51 are produced in nearly equal amounts. Like the HIV-1 p51 protein, the HTLV-1 p49 protein cannot catalyze reverse transcription by itself; RT activity requires the catalytic p66 subunit. Pol processing is controlled in part by Pol structure, since there are mutations in HIV-1 Pol that cause overprocessing and result in the accumulation of an excess of p51 (46, 47). Regardless of whether HTLV-1 is a monomer or heterodimer, the overprocessing of HTLV-1 Pol to yield

predominantly p49 and low amounts of p62 RT could underlie the relatively low polymerase activity and poor infectivity of cell-free virus particles. An important question for the future is why HTLV-1 Pol processing is not more stringently regulated to maintain higher levels of p62 RT.

Acknowledgments—We thank Dr. Péter Boross for providing the purified HTLV-1 PR, Suzanne Specht for amino acid analysis, and Dr. John Simpson for mass spectrometric analysis. We also thank Drs. Gisela Heidecker and Stephen Hughes for helpful comments and discussions.

REFERENCES

1. Jacks, T., Power, M. D., Masiarz, F. R., Luciw, P. A., Barr, P. J., and Varmus, H. E. (1988) *Nature* **331**, 280–283
2. Jacks, T., and Varmus, H. E. (1985) *Science* **230**, 1237–1242
3. Nam, S. H., Kidokoro, M., Shida, H., and Hatanaka, M. (1988) *J. Virol.* **62**, 3718–3728
4. Nam, S. H., Copeland, T. D., Hatanaka, M., and Oroszlan, S. (1993) *J. Virol.* **67**, 196–203
5. Jacks, T., Townsley, K., Varmus, H. E., and Majors, J. (1987) *Proc. Natl. Acad. Sci. U. S. A.* **84**, 4298–4302
6. Moore, R., Dixon, M., Smith, R., Peters, G., and Dickson, C. (1987) *J. Virol.* **61**, 480–490
7. Rice, N. R., Stephens, R. M., Burny, A., and Gilden, R. V. (1985) *Virology* **142**, 357–377
8. Power, M. D., Marx, P. A., Bryant, M. L., Gardner, M. B., Barr, P. J., and Luciw, P. A. (1986) *Science* **231**, 1567–1572
9. Sagata, N., Yasunaga, T., Tsuzuku-Kawamura, J., Ohishi, K., Ogawa, Y., and Ikawa, Y. (1985) *Proc. Natl. Acad. Sci. U. S. A.* **82**, 677–681
10. Sonigo, P., Barker, C., Hunter, E., and Wain-Hobson, S. (1986) *Cell* **45**, 375–385
11. Seiki, M., Hattori, S., Hirayama, Y., and Yoshida, M. (1983) *Proc. Natl. Acad. Sci. U. S. A.* **80**, 3618–3622
12. Mador, N., Panet, A., and Honigman, A. (1989) *J. Virol.* **63**, 2400–2404
13. Hruskova-Heidingsfeldova, O., Andreansky, M., Fabry, M., Blaha, L., Strop, P., and Hunter, E. (1995) *J. Biol. Chem.* **270**, 15053–15058
14. Dickson, C., and Atterwill, M. (1979) *Cell* **17**, 1003–1012
15. Dickson, C., and Peters, G. (1983) *Curr. Top. Microbiol. Immunol.* **106**, 1–34
16. Telesnitsky, A., and Goff, S. P. (1997) in *Retroviruses* (Coffin, J. M., Hughes, S. H., and Varmus, H. E., eds) 2nd Ed., pp. 121–160, Cold Spring Harbor Laboratory, Cold Spring Harbor, New York
17. Werner, S., and Wohrl, B. M. (2000) *J. Virol.* **74**, 3245–3252
18. Le Grice, S. F., Naas, T., Wohlgensinger, B., and Schatz, O. (1991) *EMBO J.* **10**, 3905–3911
19. Hostomsky, Z., Hostomska, Z., Fu, T. B., and Taylor, J. (1992) *J. Virol.* **66**, 3179–3182
20. Lederer, H., Schatz, O., May, R., Crespi, H., Darlix, J. L., Le Grice, S. F., and Heumann, H. (1992) *EMBO J.* **11**, 1131–1139
21. Jupp, R. A., Phylip, L. H., Mills, J. S., Le Grice, S. F., and Kay, J. (1991) *FEBS Lett.* **283**, 180–184
22. Rodgers, D. W., Gamblin, S. J., Harris, B. A., Ray, S., Culp, J. S., Hellmig, B., Woolf, D. J., Deboucq, C., and Harrison, S. C. (1995) *Proc. Natl. Acad. Sci. U. S. A.* **92**, 1222–1226
23. Roth, M. J., Tanese, N., and Goff, S. P. (1985) *J. Biol. Chem.* **260**, 9326–9335
24. Das, D., and Georgiadis, M. M. (2004) *Structure (Camb.)* **12**, 819–829
25. Rho, H. M., Poesz, B., Ruscetti, F. W., and Gallo, R. C. (1981) *Virology* **112**, 355–360
26. Barber, A. M., Hizi, A., Maizel, J. V., Jr., and Hughes, S. H. (1990) *AIDS Res. Hum. Retroviruses* **6**, 1061–1072
27. Johnson, M. S., McClure, M. A., Feng, D. F., Gray, J., and Doolittle, R. F. (1986) *Proc. Natl. Acad. Sci. U. S. A.* **83**, 7648–7652
28. Trentin, B., Rebeyrotte, N., and Mamoun, R. Z. (1998) *J. Virol.* **72**, 6504–6510
29. Owen, S. M., Lal, R. B., and Ikeda, R. A. (1998) *J. Virol.* **72**, 5279–5284
30. Heidecker, G., Hill, S., Lloyd, P. A., and Derse, D. (2002) *J. Virol.* **76**, 13101–13105
31. Agbuya, P. G., Sherman, N. E., and Moen, L. K. (2001) *Arch. Biochem. Biophys.* **392**, 93–102
32. Derse, D., Hill, S. A., Lloyd, P. A., Chung, H., and Morse, B. A. (2001) *J. Virol.* **75**, 8461–8468
33. Jones, M. D., and Foulkes, N. S. (1989) *Nucleic Acids Res.* **17**, 8387–8388
34. Shaffer, A. L., Wojnar, W., and Nelson, W. (1990) *Anal. Biochem.* **190**, 292–296
35. Princler, G. L., Julias, J. G., Hughes, S. H., and Derse, D. (2003) *Virology* **317**, 136–145
36. Louis, J. M., Oroszlan, S., and Tozser, J. (1999) *J. Biol. Chem.* **274**, 6660–6666
37. Kadas, J., Weber, I. T., Bagossi, P., Miklós, G., Boross, P., Oroszlan, S., and Tozser, J. (2004) *J. Biol. Chem.* **279**, 27148–27157
38. Tozser, J., Zahuczky, G., Bagossi, P., Louis, J. M., Copeland, T. D., Oroszlan, S., Harrison, R. W., and Weber, I. T. (2000) *Eur. J. Biochem.* **267**, 6287–6295
39. Entin-Meer, M., Avidan, O., and Hizi, A. (2003) *Virology* **310**, 157–162

40. Bukovsky, A., and Gottlinger, H. (1996) *J. Virol.* **70**, 6820–6825
41. Quillent, C., Borman, A. M., Paulous, S., Dauguet, C., and Clavel, F. (1996) *Virology* **219**, 29–36
42. Mariani, V. L., and Shuker, S. B. (2003) *Biochem. Biophys. Res. Commun.* **300**, 268–270
43. Tozser, J., Friedman, D., Weber, I. T., Blaha, I., and Oroszlan, S. (1993) *Biochemistry* **32**, 3347–3353
44. Schechter, L., and Berger, A. (1967) *Biochem. Biophys. Res. Commun.* **27**, 157–162
45. Wlodawer, A., and Gustchina, A. (2000) *Biochim. Biophys. Acta* **1477**, 16–34
46. Navarro, J. M., Damier, L., Boretto, J., Priet, S., Canard, B., Querat, G., and Sire, J. (2001) *Virology* **290**, 300–308
47. Abram, M. E., and Parniak, M. A. (2005) *J. Virol.* **79**, 11952–11961